

# Higgs radiation off top-antitop pairs at future Linear Colliders: a background study<sup>1</sup>

S. Moretti

*Rutherford Appleton Laboratory, Chilton, Didcot, Oxon OX11 0QX, UK.*

## Abstract

The process  $e^+e^- \rightarrow Ht\bar{t}$  can be exploited at future Linear Colliders (LCs) [1]–[2] to measure the Higgs-top Yukawa coupling. In this note, we estimate the size of the irreducible backgrounds in the channel  $Ht\bar{t} \rightarrow b\bar{b}b\bar{b}W^+W^- \rightarrow b\bar{b}b\bar{b}\ell^\pm\nu_\ell q\bar{q}'$ , for the case of a Standard Model (SM) Higgs boson with mass between 100 and 140 GeV.

## 1. Interplay of signal and backgrounds

Higgs-strahlung off top-antitop pairs [3] is the most promising channel to measure the Yukawa coupling of the top quark to a Higgs boson [4]. In the SM, the production rate of this final state at future LCs is sizable, if the energy of the latter is of the order  $\sqrt{s} \gtrsim 2m_t + M_H$ . Furthermore, the one-loop QCD corrections to  $e^+e^- \rightarrow Ht\bar{t}$  are under control [5]. Thus, in the context of simulation studies, the next thing to be assessed is the viability of the signal above the backgrounds.

The current experimental limit from LEP2 on  $M_H$  is about 95 GeV [6]. In addition, electroweak fits to precision data prefer a rather light Higgs boson, say, below 150 GeV within the SM [7]. Thus, a LC with centre-of-mass (CM) energy  $\sqrt{s} = 500$  GeV (the default of our numerical studies) represents an ideal laboratory to study  $Ht\bar{t}$  final states (as  $m_t = 175$  GeV). In the mass range  $90 \text{ GeV} \lesssim M_H \lesssim 150 \text{ GeV}$ , the dominant Higgs decay mode is  $H \rightarrow b\bar{b}$ , this being overtaken by the off-shell decay into two  $W^\pm$ 's, i.e.,  $H \rightarrow W^{+*}W^{-*}$ , only for  $M_H \gtrsim 140$  GeV [8]. Besides, the experimentally preferred channel in searching for  $t\bar{t}$  events is the semi-leptonic channel, i.e.,  $t\bar{t} \rightarrow b\bar{b}W^+W^- \rightarrow b\bar{b}\ell^\pm\nu_\ell q\bar{q}'$ , where  $\ell$  and  $\nu$  represent a lepton at high transverse momentum (used for triggering purposes) and its companion neutrino and  $q\bar{q}'$  refers to all possible combinations of light quarks. These are the signatures of Higgs and top-antitop pairs that we will concentrate on here. A study of ‘reducible’ backgrounds in the above decay channels was preliminarily presented in [9]: there, they were found to be under control after appropriate selection cuts were implemented. In this note we consider the effects of the dominant ‘irreducible’ backgrounds, i.e., those of the type [10]–[12]:

$$e^+e^- \rightarrow Ht\bar{t} \rightarrow Hb\bar{b}W^+W^- \rightarrow b\bar{b}b\bar{b}\ell^\pm\nu_\ell q\bar{q}', \quad (1)$$

<sup>1</sup>Talk given at the 2nd ECFA/DESY Study on Physics and Detectors for a Linear Electron-Positron Collider, Oxford, UK, 20-23 March 1999.

$$e^+e^- \rightarrow Zt\bar{t} \rightarrow Zb\bar{b}W^+W^- \rightarrow b\bar{b}b\bar{b}\ell^\pm\nu_\ell q\bar{q}', \quad (2)$$

$$e^+e^- \rightarrow gt\bar{t} \rightarrow gb\bar{b}W^+W^- \rightarrow b\bar{b}b\bar{b}\ell^\pm\nu_\ell q\bar{q}', \quad (3)$$

whose corresponding Feynman graphs can be found in Figs. 1–3 of Ref. [13] (the latter to be further supplemented with the  $H$ ,  $Z$  and  $g$  decay currents) as well as those of all other subleading reactions at the same perturbative orders,

$$e^+e^- \rightarrow b\bar{b}W^+W^- \rightarrow b\bar{b}b\bar{b}\ell^\pm\nu_\ell q\bar{q}', \quad (4)$$

$$e^+e^- \rightarrow Zb\bar{b}W^+W^- \rightarrow b\bar{b}b\bar{b}\ell^\pm\nu_\ell q\bar{q}', \quad (5)$$

$$e^+e^- \rightarrow gb\bar{b}W^+W^- \rightarrow b\bar{b}b\bar{b}\ell^\pm\nu_\ell q\bar{q}'. \quad (6)$$

In total, one has to consider at tree-level 350 Feynman graphs for process (4), 546 for reaction (5) and 152 for case (6), each number including the graphs associated to (1)–(3). Their computation has been accomplished by using helicity amplitude techniques to evaluate the complete  $2 \rightarrow 8$  body reactions, without any factorisation of production and decay processes [13].

## 2. Cross sections

If one does assume the mentioned Higgs and top-antitop decay modes, then signal events can be searched for in data samples made up by four  $b$  quark jets, two light quark jets, a lepton and a neutrino. In other terms, a ‘ $4b + 2 \text{ jets} + \ell^\pm + E_{\text{miss}}$ ’ signal, with  $\ell = e, \mu, \tau^2$ . Fig. 1 presents the production cross sections for the leading subprocesses (1)–(3) as well as those for the complete ones (4)–(6). From there, two aspects emerge. On the one hand, the QCD processes are always dominant, whereas the interplay between the other two depends upon the Higgs mass value. On the other hand, the bulk of the cross sections of processes (4)–(6) comes from (1)–(3) with the only exception of the QCD case. The increase of the QCD rates seen in the figure is mainly due to the large amount of gluon radiation off  $b$  (anti)quarks produced in ‘radiative’  $t\bar{t}$  decays [12]: i.e., via  $t\bar{t} \rightarrow b\bar{b}W^+W^- \rightarrow gb\bar{b}W^+W^-$ , with the gluon eventually yielding  $b\bar{b}$  pairs: see Fig. 2. However, it is instructive to further explore the background effects in the case of  $Hb\bar{b}W^+W^-$  events. This is done in Fig. 3, where we have distinguished between subprocess (1) and four sizable components of (4), i.e., the cases proceeding via intermediate states of the following forms: (4a)  $Ht\bar{b}W^- + \text{c.c.}$ , (4b)  $HZW^+W^-$ , (4c)  $H\gamma W^+W^-$ , (4d)  $HHW^+W^-$ , (4e) all remaining interferences. A notable aspect in Fig. 3 is the taking over of the ‘single-top’ production rates (4a) respect to the ‘double-top’ ones (1) for large Higgs masses, because of the strong phase space suppression on the latter when  $M_H$  approaches  $\sqrt{s} - 2m_t$ . Besides, (4a) events carry the same Yukawa dependence as (1), see Fig. 4, thus they should rather be regarded as an additional contribution to the top-Higgs Yukawa signal, these two mechanisms being somehow complementary with respect to the  $M_H$  dependence.

---

<sup>2</sup>We include  $\tau$ ’s to enhance the signal rate, assuming that they are distinguishable from quark jets.

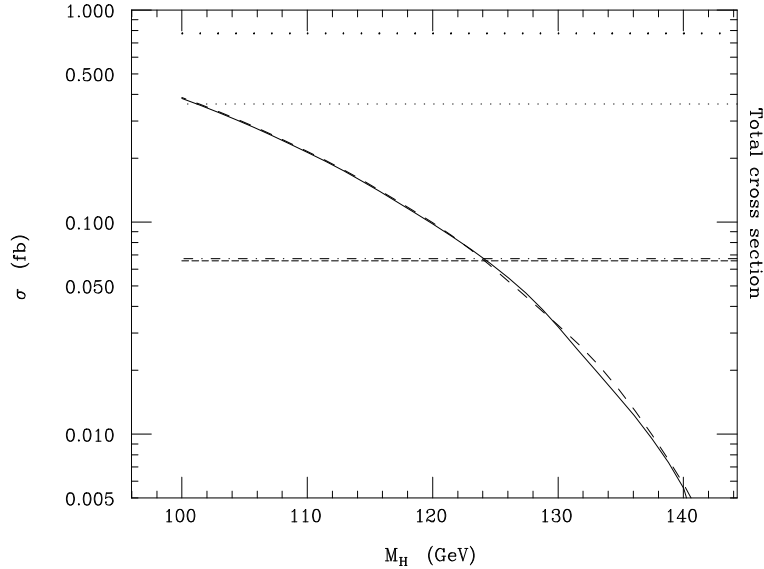


Figure 1: Cross sections for the following processes (see the text): (1) (solid), (2) (dashed), (3) (fine-dotted), (4) (long-dashed), (5) (dot-dashed) and (6) (dotted).

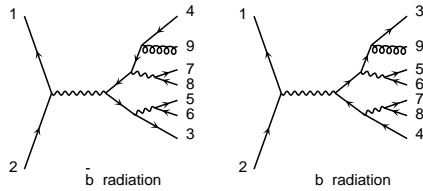


Figure 2: The diagrams responsible for radiative top-antitop decays in process (6).

As one of the  $b\bar{b}$  pairs in the final state would naturally resonate at  $M_H$ , at  $M_Z$  or logarithmically increase at low mass, for processes (1), (2) and (3), respectively, we investigate the di-jet mass spectra that can be reconstructed from the four  $b$  quarks in the ‘ $4b + 2 \text{ jets} + \ell^\pm + E_{\text{miss}}$ ’ signature. Since we do not assume any jet-charge determination of the  $b$  jets and consider negligible the mis-tagging of light-quark jets as heavy ones, six such combinations can be built up. We distinguish among these by ordering the four  $b$  jets in energy (i.e.,  $E_1 > E_2 > E_3 > E_4$ ), in such a way that the  $2b$  invariant mass  $m_{ij}$  refers to the  $ij$  pair (with  $i < j = 2, 3, 4$ ) in which the  $i$ -th and  $j$ -th most energetic particles enter. In Fig. 5 (top), one can appreciate the ‘resonant’ shapes around  $M_H$  and  $M_Z$  in all  $ij$  cases. As for the ‘divergence’ in the  $g \rightarrow b\bar{b}$  splitting of the QCD process, this can easily be spotted in the case  $ij = 34$ . In the end, the  $2b$  mass spectra look rather promising as a mean of reducing both backgrounds (2)–(3). By requiring, e.g.,  $m_{34} > 50$  GeV, one would vigorously reduce the latter; similarly, by imposing, e.g.,  $|m_{14} - M_Z| > 15$  GeV one would reject the former considerably.

An alternative way of looking at the same phenomenology is by studying the energy

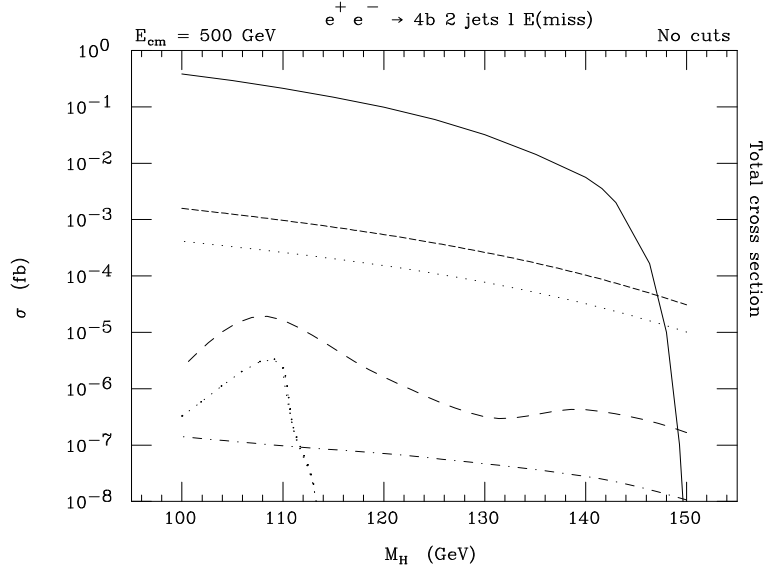


Figure 3: Cross sections for the (1) subprocess (solid) and the following other components of the full reaction (4) (see the text): (4a) (dashed), (4b) (dotted), (4c) (long-dashed), (4d) (dot-dashed) and (4e) (fine-dotted).

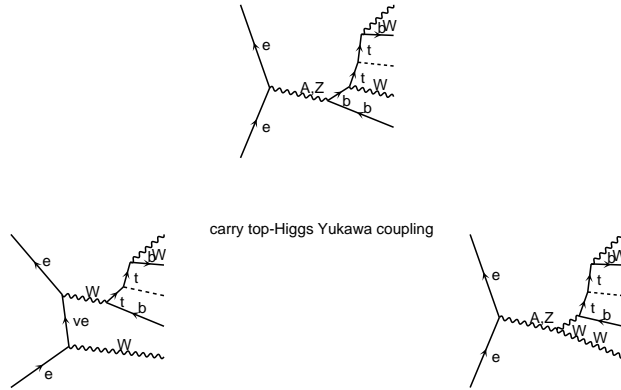


Figure 4: The diagrams responsible for single-top events in process (4).

spectra of the four  $b$  quarks. In fact, the larger value of  $M_H$ , as compared to  $M_Z$ , should boost the  $b$  quarks generated by the Higgs boson towards energies higher than those achieved in the  $Z$  decays. Conversely, the energy of the  $b$  quarks emerging from the two remaining unstable particles, top and anti-top quarks, should be softer in the first case. Following similar arguments, one should expect the hardest(softest)  $b$  (anti)quark from gluon events to actually be the hardest(softest) of all cases (1)–(3). Recalling that the two most energetic  $b$ 's seldom come from a  $H$ ,  $Z$  or  $g$  splitting, the above kinematic features are clearly recognisable in Fig. 5 (bottom). Therefore, the energy spectra too are useful in disentangling Higgs events. If one imposes, e.g.,  $E_1 < 100$  GeV and  $E_4 > 50$  GeV,

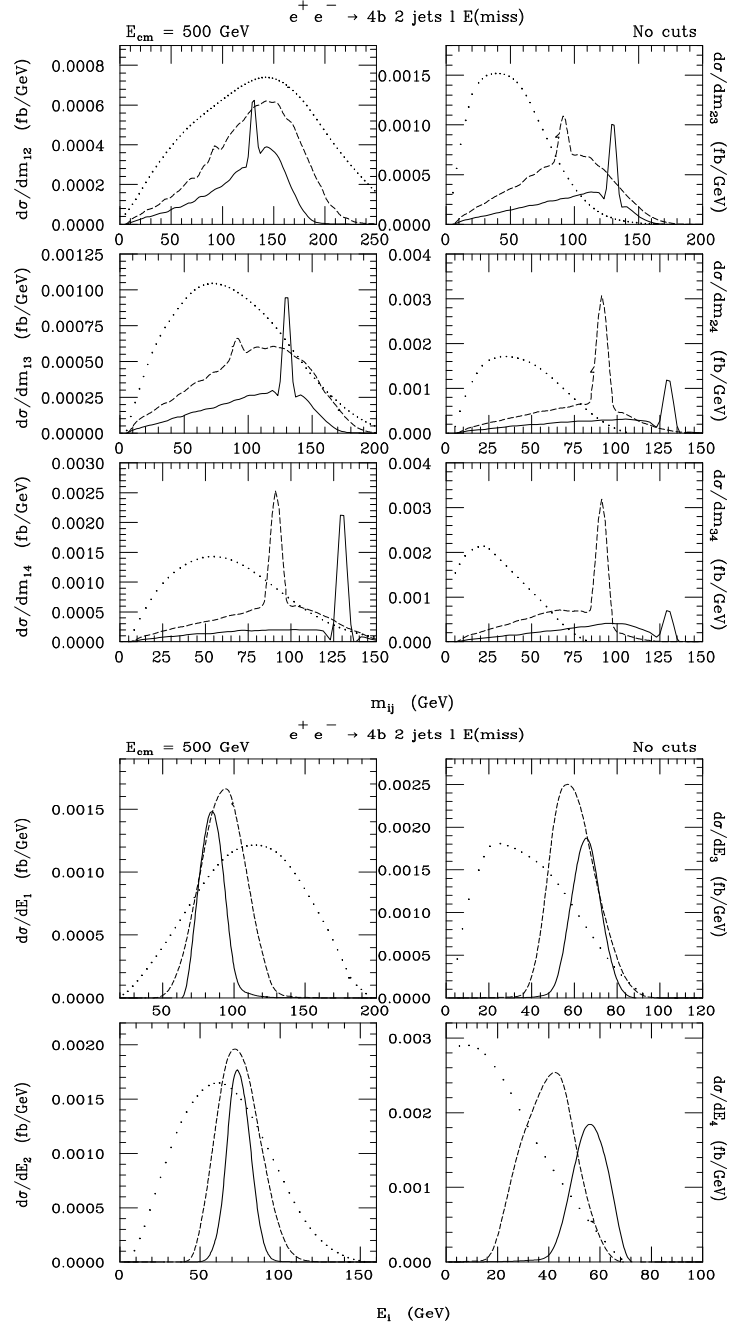


Figure 5: Differential distributions in invariant mass (top) and energy (bottom) of the energy-ordered  $b$  jets for the following processes (see the text): (1) (solid), (2) (dashed) and (3) (dotted). (Note that the rates of reaction (3) have been divided by three for readability.)

both  $Z$  and gluon events can be strongly depleted, at a rather low cost for the signal.

### 3. Conclusions

Taking into account our results, we believe that the study of the Higgs-top Yukawa coupling at future  $e^+e^-$  accelerators, running at 500 GeV or higher, can be pursued by means of the Higgs-strahlung process  $e^+e^- \rightarrow Ht\bar{t}$ . In particular, the irreducible backgrounds can be controlled in the decay channels  $t\bar{t} \rightarrow b\bar{b}W^+W^- \rightarrow b\bar{b}\ell^\pm\nu_\ell q\bar{q}'$  and  $H \rightarrow b\bar{b}$ , for  $M_H \lesssim 140$  GeV. Those presented here are predictions obtained at parton level only, though with an advanced perturbative treatment based on  $2 \rightarrow 8$  body processes. They should be complemented with others at a more phenomenological level, also including fragmentation/hadronisation and detector effects. Indeed, several progress has recently been made in this respect [14], which confirmed the feasibility of this kind of analyses.

Acknowledgements We thank the conveners of the top working group for the stimulating environment they have been able to create during the workshops.

### References

- [1] Proceedings of the Workshop ‘ $e^+e^-$  Collisions at 500 GeV. The Physics Potential’, Munich, Annecy, Hamburg, ed. P.M. Zerwas, DESY 92-123 A/B/C, 1992-1993.
- [2] Proceedings of the Workshop ‘Physics with  $e^+e^-$  Colliders’, Annecy, Gran Sasso, Hamburg, ed. P.M. Zerwas, DESY 97-100, 1997 [*Phys. Rep.* **299** (1998) 1].
- [3] A. Djouadi, J. Kalinowski and P.M. Zerwas, *Mod. Phys. Lett.* **A7** (1992) 1765; *Z. Phys.* **C54** (1992) 255.
- [4] W. Bernreuther *et al.*, in [1], part A, page 255; G. Bagliesi *et al.*, *ibidem*, page 327.
- [5] S. Dawson and L. Reina, *Phys. Rev.* **D59** (1999) 054012; S. Dittmaier, M. Krämer, Y. Liao, M. Spira and P. M. Zerwas, *Phys. Lett.* **B441** (1998) 383.
- [6] See, e.g.: <http://www.cern.ch/LEPHIGGS/>.
- [7] See, e.g.: <http://www.cern.ch/LEPEWWG/>.
- [8] Z. Kunszt, S. Moretti and W.J. Stirling, *Z. Phys.* **C74** (1997) 479.
- [9] G. Merino, talk given at the 4th workshop of the ‘2nd Joint ECFA/DESY Study on Physics and Detectors for a Linear Electron-Positron Collider’, Oxford, UK, 20-23 March 1999.
- [10] K.J.F. Gaemers and G.J. Gounaris, *Phys. Lett.* **B77** (1978) 379.
- [11] K. Hagiwara, H. Murayama and T. Watanabe, *Nucl. Phys.* **B367** (1991) 257.
- [12] L.H. Orr, T. Stelzer and W.J. Stirling, *Phys. Lett.* **B354** (1995) 442.
- [13] S. Moretti, *Phys. Lett.* **B452** (1999) 338.
- [14] A. Juste and G. Merino, preprint October 1999, [hep-ph/9910301](http://arxiv.org/abs/hep-ph/9910301); H. Baer, S. Dawson and L. Reina, *Phys. Rev.* **D61** (2000) 013002.